The multiple orientation relationships and morphology of beta phase in Al-Mg-Si-Cu alloy

Accepted Manuscript

The multiple orientation relationships and morphology of β' phase in Al-Mg-Si-Cu alloy

Yaoyao Weng, Zhihong Jia, Lipeng Ding, Shinji Muraishi, Xiaozhi Wu, Qing Liu

PII: S0925-8388(18)32578-7

DOI: 10.1016/j.jallcom.2018.07.077

Reference: JALCOM 46793

To appear in: *Journal of Alloys and Compounds*

Received Date: 18 February 2018

Revised Date: 5 July 2018

Accepted Date: 7 July 2018

Please cite this article as: Y. Weng, Z. Jia, L. Ding, S. Muraishi, X. Wu, Q. Liu, The multiple orientation relationships and morphology of β' phase in Al-Mg-Si-Cu alloy, *Journal of Alloys and Compounds* (2018), doi: 10.1016/j.jallcom.2018.07.077.

The multiple orientation relationships and morphology of β´ phase in Al-Mg-Si-Cu alloy

Yaoyao Weng[a, e], Zhihong Jia[a,b,*], Lipeng Ding[c, d], Shinji Muraishi[e], Xiaozhi Wu[f], Qing Liu[a]

[a] *College of Materials Science and Engineering, Chongqing University, Chongqing 400044, China*

[b] *Electron Microscopy Center of Chongqing University, Chongqing 400044, China*

[c] *Université catholique de Louvain, Institute of Mechanics, Materials and Civil Engineering, IMAP, 1348 Louvain-la-Neuve, Belgium*

[d] *Electron Microscopy for Materials Science (EMAT), Department of Physics, University of Antwerp, Groenenborgerlaan 171, B-2020*

[e] *Department of Metallurgy and Ceramics Science, Tokyo Institute of Technology, 2-12-1 Meguro-ku, Tokyo 152-8552, Japan*

[f] *College of Physics, Chongqing University, Chongqing 400044 China*

Abstract

The orientation relationships (ORs), segregation behavior and morphologies of β´ precipitate in an over-aged Al-Mg-Si-Cu alloy are systematically characterized by atomic resolution high-angle annular dark-field scanning transmission electron microscopy (HAADF-STEM). Six different ORs and two morphologies, i.e. rod- and lath-like are revealed for β´ precipitates, and Cu segregation at the β′/α-Al interface is observed in all these precipitates. The rod-like β´ precipitate has multiple β´-angles ranging from 6.1^{o} to 14.1^{o} and non-uniform Cu segregation at the β′/α-Al interface, while the lath-like β´ precipitate has a constant β´-angle of 0^{o} and a periodic Cu segregation. These different ORs are explained to be attributable to the rotation of QP lattice, a near-hexagonal network of Si columns formed within β´ precipitates, which causes different lattice matching of β′ with α-Al lattice. These findings provide new insights in controlling the precipitation hardening and mechanical properties of this type of alloys.

Keywords:

Aluminum alloy; Precipitates; Atomic resolution HAADF-STEM; Orientation relationship; Cu segregation;

1. Introduction

Heat-treatable Al-Mg-Si (6xxx) alloys are widely used in the automotive and aircraft industries due to their high strength/weight ratio, good formability and corrosion resistance. These alloys are featured by the remarkable strengthening potential due to the formation of large number of nano-sized metastable precipitates during heat treatment. The crystal structure of precipitates and their evolution in Al-Mg-Si alloys had been extensively investigated in recent years, and the precipitation sequence of Al-Mg-Si alloys is reported as follows [1-3]:

SSSS → Atomic clusters → GP zones → β″ → β′, U1, U2, B′ → β, Si

Where SSSS stands for super-saturated solid solution. The needle-like β″ phase has monoclinic structure and responsible for the peak hardness of Al-Mg-Si alloys [4]. The β′ (Mg_9Si_5) phase is mainly reported to have rod-shaped morphology with its long axes parallel to $<001>_{\alpha}$. Previous studies reported that the β′ phase has hexagonal structure, space group $P6_3/m$, with unit cell parameters a = 0.715 nm and c = 1.215 nm. The orientation relationship (OR) between β′ phase and α-Al matrix is generally accepted as: $[0001]_{\beta'}$ // $[001]_{\alpha}$, $<2\bar{1}\bar{1}0>_{\beta'}$ // $<\bar{3}\,10>_{\alpha}$ [5]. The metastable U1, U2 and B′ precipitates come in the shapes of needles/rods/laths and are also known as Type-A, Type-B and Type-C, respectively [2, 6]. They form mostly together with β′ phases upon over-ageing treatment in the Si-rich Al-Mg-Si alloys. The equilibrium β (Mg_2Si) phase can be plate or cube-shaped.

Cu addition alters the precipitation sequence as follows [7]:

SSSS → Atomic clusters → GP zones → β″, QP1, QP2, C → Q′, QP2, C → Q, Si.

Cu addition suppresses the formation of β″ and causes other Cu-containing metastable precipitates such as QP1, QP2 and C formed at the peak hardness condition. The disordered QP1 and QP2 phases are precursor of Q′ phase. The QP2 phase is similar to the L phase used in published literatures [8, 9]. These metastable precipitates could transform to equilibrium Q phases after very long aging treatment.

The OR between precipitate and its surrounding matrix plays a significant role in determining the morphology evolution and strengthening ability of precipitates. Numerous

reports about the OR of various precipitates in Al-Mg-Si(-Cu) alloys have been published in recently years. The ORs between various precipitates and α-Al matrix in these alloys are summarized in Table 1. It seems that the ORs of precipitates in Al-Mg-Si(-Cu) alloys have been already well resolved. Recently, M. Fiawoo et al. [10] revealed that multiple ORs are found between the Q precipitate and its surrounding α-Al matrix in A6111 (Al-Mg-Si-Cu) alloy, and six different ORs are identified by atomic resolution high-angle dark-field scanning transmission electron microscopy (HAADF-STEM). L.P. Ding et al. [11] further revealed the relationship between morphology and OR of Q′ phase in Al-Mg-Si-Cu alloys, and indicated that the rod Q′ phase has multiple ORs with Q′-angle ranging from 3.4° to 15.5°, while the lath Q′ phase has a conventional OR with a constant Q′-angle of 11°. These issues arouse the multiple ORs of β′ precipitates in Al-Mg-Si alloys, which has not been considered by other researchers before.

The strengthening potential of heat-treatment Al-Mg-Si alloy is strongly influenced by the size, morphology, distribution and OR of precipitates, and thus any improved understanding of the crystallography and formation mechanism of precipitates is of importance for improving properties of these alloys. The driving force for morphology evolution of precipitate stems from the anisotropic misfit strain and the orientation dependence of interface energy. The segregation of solute atoms at the precipitate/matrix interface could accommodate the elastic strain normal to the habit plane [12], and the OR of precipitate plays a significant role in determining the misfit strain. Thus the solute segregation and OR of precipitates could influence the morphology evolution and strengthening potential of precipitates. A detailed interaction mechanism between the OR, interfacial behavior and morphology evolution of precipitates is still not clear. Besides, the influence of Cu on the interfacial structure of β′ precipitate is poorly studied for Al-Mg-Si-Cu alloys. In the present study, by means of atomic resolution HAADF-STEM, the multiple ORs and morphologies of β′ precipitate were revealed in an Al-Mg-Si-Cu alloy, and the correlation among the OR, solute segregation and morphology of β′ precipitates was systematically investigated. Besides, the multiple ORs of other precipitates in Al-Mg-Si(-Cu) alloys are also discussed.

2. Experimental

An alloy with chemical composition of 1.13 Mg, 0.71 Si, 0.01 Cu, 0.11 Fe and 0.06 Mn (wt. %) was used for all the experiments. Other impurities had a total content less than 0.01 wt. %. The cold rolled alloy was solution heat treated at 570 ^{o}C for 20 min, water quenched and aged at 170 ^{o}C for 1 month, which corresponds to the over-aging stage. The TEM/STEM samples were prepared by electro polishing using a Struers TenuPol-5 machine with an electrolyte of 1/3 HNO_3 in methanol at a temperature of about -30 °C. Precipitate observations and EDS analysis were carried out in a FEI Titan G2 60–300 ChemiSTEM, equipped with a Cs probe corrector and a Super-X EDS with four windowless silicon-drift detectors and operated at 300 kV. The probe diameter was 0.08 nm, and a 15 mrad convergence semi-angle and a spot size 7 were used for HAADF imaging and EDS data collection in STEM mode. All TEM/STEM images in this work were taken along a $<001>_{\alpha}$ zone axis, and the HAADF-STEM images were Fourier filtered with an aperture encompassing all the visible spots in the Fourier transform in order to remove noise.

3. Results

Fig. 1 (a) shows a bright-field TEM image of the Al-Mg-Si-Cu alloy aged at 170 °C for 1 month. It could be seen that rod- and lath-like β′ precipitates were homogenously distributed within the α-Al matrix. The shape of precipitates, i.e. rod and lath, is separated by the aspect ratio of cross-section of precipitates, which is determined as the quotient of the largest precipitate dimension and the width measured orthogonal to this dimension. Precipitates with aspect ratio smaller than 2 are denoted as rod-shaped, and those precipitates with aspect ratio larger than 2 are labelled as lath-shaped. The rod-like β′ accounts for 84% of the total number of β′ precipitates by statistical analysis of five TEM images including more than 100 individual precipitates. Fig. 1 (b, c) show the HAADF-STEM image and the corresponding fast Fourier transform (FFT) pattern of cross-section of a rod-like β′ precipitate, respectively. All atomic columns can be clearly resolved in the HAADF-STEM image. A near-hexagonal network of Si columns, called the QP lattice [7] (which was also named as Si-network [13]), was observed in the β′ precipitate (green lines in Fig. 1 (b)). The hexagonal unit cell of the β′

phase was outlined by red lines in Fig. 1 (b), and the lattice parameters were measured as $a_{\beta'}$ = 0.715 nm and $c_{\beta'}$ = 1.215 nm from the corresponding FFT pattern. The OR between β′ phase and α-Al matrix could be identified as: $[0001]_{\beta'}$ // $[001]_{\alpha}$, $<2\bar{1}\bar{1}0>_{\beta'}$ // $<1\bar{3}0>_{\alpha}$, (OR0). The lattice parameters and OR have been reported in literatures [5, 14]. The angle of $<11\bar{2}0>_{\beta'}$ with its nearest $<100>_{\alpha}$ which termed as "β′-angle", was measured as 11.6°. The interatomic row distance of a $<2\bar{1}\bar{1}0>_{\beta'}$ direction is 0.619 nm and the corresponding atomic row distance of α-Al is 0.640 nm along the $<1\bar{3}0>_{\alpha}$ direction, so the lattice misfit value between β′ phase and α-Al matrix along the parallel direction of $<2\bar{1}\bar{1}0>_{\beta'}$ // $<1\bar{3}0>_{\alpha}$ is calculated to be 3.28%, implying semi-coherent lattice matching in this direction. The misfit dislocations can be observed in the semi-coherent β′/α-Al interface, as shown in supplementary Fig. S1.

Fig. 2 shows four HAADF-STEM images of cross-section of the rod-like β′ phases. Except for the OR0, four different ORs were detected for these rod-like phases. The first group, OR1, had its measured β′-angle value of ~6.1°, suggesting that $<2\bar{1}\bar{1}0>_{\beta'}$ is parallel to $<4\bar{9}0>_{\alpha}$ (Fig. 2 (a-c)). The second group, OR2, had a β′-angle of ~9.4°, and can be defined as $[0001]_{\beta'}$ // $[001]_{\alpha}$ and $<2\bar{1}\bar{1}0>_{\beta'}$ // $<3\bar{8}0>_{\alpha}$ (Fig. 2 (d-f)). The rod-like β′ phases in OR groups 3 and 4 had β′-angles of ~12.5° and ~14.1°, respectively. These groups can be expressed as $[0001]_{\beta'}$ // $[001]_{\alpha}$, $<11\bar{2}0>_{\beta'}$ // $<9\bar{2}0>_{\alpha}$ (OR3) and $[0001]_{\beta'}$ // $[001]_{\alpha}$, $<11\bar{2}0>_{\beta'}$ // $<4\bar{1}0>_{\alpha}$ (OR4), respectively. A common QP lattice was observed in all these β′ phases, as marked by the green lines in Fig. 2 (a). Besides, few solute atoms were non-uniformly segregated at the rod-like β′/α-Al interfaces.

Fig. 3 shows the HAADF-STEM image and STEM-EDS mapping of cross-section of a rod-like β′ phase. Owing to the higher atomic number of Cu (Z = 29) than that of other elements (Z = 14 for Si, 13 for Al and 12 for Mg), Cu atomic columns can be identified as brightest dots relative to any other columns in the HAADF-STEM images. From the STEM-EDS images, it could be seen that the β′ phase mainly consists of Mg and Si elements. Cu element can be observed at the interface of β′, while low signal of Fe and Mn elements are also detected, really close to noise level. In combination of HAADF-STEM and STEM-EDS mapping, it was identified that Cu atomic columns were non-uniformly segregated at the rod β′/α-Al interface, and no Cu atomic column was observed in the interior of β′ phase. Enlarged HAADF-STEM image and illustration schematic of the Cu segregation for a rod-like β′ phase

are shown in Fig. 6 (a-c). It could be seen that these segregated Cu atoms mainly occupied two positions at the β′/α-Al interface: the Al atoms in FCC matrix nearest to QP lattice and the Si atoms in QP lattice for β´ phases.

Fig. 4 shows two HAADF-STEM images of cross-section of the lath-like β′ phases. It could be seen that the lath-like β′ phases had a constant OR with the β′-angle of 0^o (OR5) and the OR5 can be expressed as: $[0001]_{\beta'}$ // $[001]_\alpha$, $<2\bar{1}\bar{1}0>_{\beta'}$ // $<100>_\alpha$ and $<01\bar{1}0>_{\beta'}$ // $<010>_\alpha$. The interatomic row distance of lath-like β´phase along a $[01\bar{1}0]_{\beta'}$ direction is 1.238 nm and the corresponding atomic row distance of α-Al is 1.215 nm along the $[010]_\alpha$ direction, so the lattice misfit between lath-like β´phase and α-Al matrix along the parallel directions of $[01\bar{1}0]_{\beta'}$ // $[010]_\alpha$ is calculated to be 1.86%, while the misfit along the $[2\bar{1}\bar{1}0]_{\beta'}$ // $[100]_\alpha$ is 13.33%. This means that the lath-like β´ phase is coherent with the α-Al matrix on the $(100)_\alpha$ habit plane while is partially coherent with the α-Al matrix on the $(010)_\alpha$ plane. Different from the rod-like β′ phases, the lath-like β′ phases had a constant $\{100\}_\alpha$ habit plane, and a periodic solute segregation was observed at the coherent β′/α-Al interfaces. Fig. 5 shows the HAADF-STEM image and STEM-EDS mapping of cross-section of a lath-like β′ phase. Similar as rod-like β′ phases, the lath-like β´ phase mainly consists of Mg and Si elements, and some Cu atoms were observed at the interface. The quantitative composition analysis in three different areas, i.e. β´/α-Al interface, β´ precipitate and α-Al matrix presented in supplementary Fig. S2, shows the Cu concentration in the interface (3.6 at.%) is much higher than that of the interior of precipitate (0 at.%) and matrix (0.5 at.%), which clearly indicates the segregation of Cu atoms at the β´/α-Al interface. Enlarged HAADF-STEM image and illustration schematic of the Cu segregation for a lath-like β′ phase are shown in Fig. 6 (d-f), the lath-like β′ had a periodic Cu segregation at the β′/α-Al interface, and most of the Cu segregation spacing (d_{Cu}) can be measured as 6 times of the Al atomic column distance in the matrix ($6d_{Al}$). The segregated Cu atoms occupied the position of Al atoms in FCC matrix which is nearest to Si atoms at the interface.

Despite significant variations in the measured values of β′-angle for the rod-like β′ phase, ranging from ~0^o to 14.1^o, the distribution of β′-angle values was not uniform in this variation range, which is similar to the phenomenon reported in Q phase by M. Fiawoo et al. [10] and Q′ phase by L.P. Ding et al. [11]. The β′-angle distribution of β′ phases in the Al-Mg-Si-Cu

sample is counted and shown in Fig. 7. Compared with the OR1 (~6.1^{o}) and OR2 (~9.4^{o}), β′ phases are prone to form the OR3 (~12.5^{o}) and OR4 (~14.1^{o}). Besides, the frequency of β′ phase in OR5 was 16%.

The correlation among the six ORs is illustrated schematically by the stereographic projection shown in Fig. 8 (a). It shows that all the six ORs are closely related and may be described by simple rigid-body rotations about $[0001]_{\beta'}$. In order to clarify the relationship between the OR and morphology of β′ phases, more than 50 individual β′ phases were measured and the β′-angle as a function to the aspect ratio of the cross-section of each β′ phase is shown in Fig. 8 (b). It could be seen that the rod-like β′ phases with aspect ratio between 1-2 had a continuous or near-continuous range of ORs with the β′-angle ranging from 6.1^{o} to 14.1^{o}, while all the lath-like β′ phases with aspect ratio larger than 2 had a constant β′-angle of 0^{o}. This implies that the lath-like β′ has a constant OR, while multiple ORs are presented for the rod-like β′.

4. Discussion

Understanding the correlation among the OR, solute segregation and morphology of precipitates should firstly unveil the lattice misfit between the β′ phase and α-Al matrix. The morphology of precipitate is mainly determined by the anisotropic misfit strain and the interface energy. In the over-aged stage, the morphology evolution and growth kinetic of precipitates are significantly influenced by the strain energy [15]. The growth of semi-coherent planes is suppressed due to the growth ledge to a low-energy coherent interface with a high energetic cost. Instead, growth ledge to a semi-coherent interface is favored, which strongly affects the precipitate morphology [16-19]. So the anisotropic lattice misfit in the cross-section of β′, determined by the OR between β′ and α-Al matrix, is crucial to explain the morphology variations of β′ phase. The lattice misfits of different ORs between β′ and α-Al matrix were calculated as listed in Table 2. As all β′ phases have perfectly coherent interface along $[0001]_{\beta'}$ // $[001]_{\alpha}$ direction, lattice misfit in two perpendicular directions of cross-section of β′, such as $[2\bar{1}\bar{1}0]_{\beta'}$ and $[10\bar{1}0]_{\beta'}$ were calculated. For the β′ phases with OR0 to OR4, the misfit values along the $[2\bar{1}\bar{1}0]_{\beta'}$ and $[10\bar{1}0]_{\beta'}$ are similar, implying the unobvious

anisotropic misfit strain in these precipitates. This small anisotropic misfit strain leads to the almost uniform growth for β′ cross-section and thus the rod-shaped precipitates formed. For the β′ phase with OR5, the lattice misfit along the $[2\bar{1}\bar{1}0]_{\beta'}$ // $[100]_{\alpha}$ was small as 1.89%, while the lattice misfit along the $[10\bar{1}0]_{\beta'}$ // $[010]_{\alpha}$ was measured as 13.33%. The large anisotropic lattice misfit produces a lath shape of precipitates. The majority of β′ precipitates were in the groups of OR3 and OR4, which is due to the low lattice matching of these ORs minimizing the free energy of precipitates, while the OR1 and OR2 with high lattice matching are not the favorable OR of β′.

Different Cu segregation was found at the rod and lath β′/α-Al interfaces. For the lath-like β′ with a $\{100\}_{\alpha}$ habit plane, this phase is coherent with the α-Al matrix on the $(100)_{\alpha}$ plane while is partially coherent on the $(010)_{\alpha}$ plane, suggesting that the $(010)_{\alpha}$ plane is elastically strained. Schematic illustration of the interface is showed in Fig. 9. Since the Cu atom has a smaller atomic radius (0.128 nm) than Al atom (0.143 nm), substitution of Cu for Al on the coherent $(100)_{\alpha}$ plane can accommodate the strain stress in the partially coherent $(010)_{\alpha}$ interface, which is perpendicular to the habit plane, thus the strain energy of $(010)_{\alpha}$ interface is reduced. The periodic segregation of Cu is supposed in association with the periodic arrangement of β′ unit cell and the strong interaction between the segregated Cu atoms and the Si atoms within the precipitate [20]. While for the rod-like β′, the anisotropic misfit values are ranging from 0.75% to 5.62%, smaller than that of the lath-like β´ (11.47%), as indicated in Table 2. Cu atoms randomly segregate at the rod-like β′/α-Al interface due to the relative isotropy of misfit stain. Therefore, Cu segregation at β´/α-Al interfaces could accommodate the strain energy, and the different Cu segregation behavior was related to the anisotropic misfit strain of β′ phases.

The presence of multiple ORs is the crucial reason for the different morphology and Cu segregation behavior in the β′ precipitates. The multiple ORs are mainly determined by the atomic-scale structure of precipitates, and understanding the mechanism of multiple ORs of β′ can shed light on the OR stability of other precipitates in Al-Mg-Si(-Cu) alloys, such as β″, Q′, QP2, U1 and U2. It was recently discovered that all metastable precipitates in the Al-Mg-Si(-Cu) alloys are structurally connected through a common QP lattice [7] (which is also named as Si-network by C.D. Marioara [9, 13]) with a projected near hexagonal

symmetry of a = b ≈ 0.4 nm, c = n × 0.405 nm, with c being parallel to the needle/rod/lath direction. These precipitates are basically different arrangements of Al, Mg and Cu atomic columns on the QP lattice, as viewed along its c direction. An exception from the above precipitates is the β″ phase, which has a distorted QP lattice due to the full coherency with α-Al matrix. The QP lattice, acts as the stable skeleton of precipitates, plays an important role in determining the OR of precipitates in Al-Mg-Si(-Cu) alloys [21]. As listed in Table 1, besides the β′ phase, other precipitates such as Q′, U1 and U2 phases were also observed with multiple ORs. M. Fiawoo et al. [10] firstly revealed six different ORs for the Q phase, ranging from 3.4^{o} to 15^{o}. Multiple ORs of U1 and U2 phases are also reported. From the illustration of crystal structure of these precipitates presented in Fig. 10, the main common point for the β′, Q′, U1 and U2 phases is the presence of hexagonal QP lattice, which determines the OR of these precipitates. The rotation of QP lattice along the long axes of the laths/rods results in different ORs of precipitates which have relatively similar misfit values and hence are energetically similar, allowing several ORs to form in practice. Similar multiple ORs have also been reported for rod-shaped β′ phase in Mg-Zn alloys [22]. While for the β″ without QP lattice, the rotation of precipitate is not possible, and thus leads to a constant OR of β″. An exception is the QP2 phase, which contains QP lattice but observed to have a constant OR. The main reason for the constant OR of QP2 phase is that the QP lattice is locked by the substructure of Cu sub-unit clusters [7]. The variations of morphology and OR in β′ phases observed in the present work would affect the precipitation hardening of Al-Mg-Si alloys. Understanding the interaction mechanism among OR, solute segregation and morphology of precipitates provides new insights in controlling the precipitation hardening and mechanical properties of this type of alloys.

5. Conclusions

(1) The rod- and lath-like β´ precipitates with six different ORs are revealed, and Cu segregation at the β′/α-Al interfaces is observed in all β′ precipitates. The segregated Cu atoms mainly occupy two positions at the interface: the Al sites in FCC matrix nearest to QP lattice composed of the Si sites in β´ phases.

(2) The rod-like β′ precipitate has a multiple β′-angle range from 6.1° to 14.1° and non-uniform Cu segregation, while the lath-like β′ precipitate has a constant β′-angle of 0° and a periodic Cu segregation at the coherent interface. These different ORs are explained to be attributable to the rotation of QP lattice formed within β′ precipitates, which causes different lattice matching of β′ and α-Al matrix.

Acknowledgments

This work was supported by the Fundamental Research Funds for the Central Universities of China (Grant No. 2018CDJDCL001910611 and No. 2017CDJQJ308822), the Foundation for Innovative Research Groups of the National Natural Science Foundation of China (Grant No. 51421001) and the program of China Scholarships Council (No. 201706050125).

References

[1] G.A. Edwards, K. Stille, G.L. Dunlop, M.J. Couper, Acta Mater. 46 (1998) 3893-3904.

[2] K. Matsuda, Y. Sakaguchi, Y. Miyata, Y. Uetani, T. Sato, S.I. A. Kamio, J. Mater. Sci. 35 (2000) 179-189

[3] S.J. Andersen, C.D. Marioara, A. Frøseth, R. Vissers, H.W. Zandbergen, Mater. Sci. Eng. A 390 (2005) 127-138.

[4] S.J. Andersen, H.W. Zandbergen, J. Jansen, C. TrÆholt, U. Tundal, O. Reiso, Acta Mater. 46 (1998) 3283-3298.

[5] R. Vissers, M.A. van Huis, J. Jansen, H.W. Zandbergen, C.D. Marioara, S.J. Andersen, Acta Mater. 55 (2007) 3815-3823.

[6] S.J. Andersen, C.D. Marioara, R. Vissers, A. Frøseth, H.W. Zandbergen, Mater. Sci. Eng. A 444 (2007) 157-169.

[7] L. Ding, Z. Jia, J.-f. Nie, Y. Weng, L. Cao, H. Chen, X. Wu, Q. Liu, Acta Mater. 145 (2018) 437-450.

[8] M. Torsæter, W. Lefebvre, C.D. Marioara, S.J. Andersen, J.C. Walmsley, R. Holmestad,

Scripta Mater. 64 (2011) 817-820.

[9] C.D. Marioara, S.J. Andersen, T.N. Stene, H. Hasting, J. Walmsley, A.T.J. Van Helvoort, R. Holmestad, Philos. Mag. 87 (2007) 3385-3413.

[10] M. Fiawoo, X. Gao, L. Bourgeois, N. Parson, X.Q. Zhang, M. Couper, J.F. Nie, Scripta Mater. 88 (2014) 53-56.

[11] L. Ding, Z. Jia, Y. Weng, Y. Liu, S. Wu, Q. Liu, Mater. Charact. 118 (2016) 279-283.

[12] K. Matsuda, D. Teguri, Y. Uetani, T. Sato, S. Ikeno, Scripta Mater. 47 (2002) 833-837.

[13] T. Saito, C.D. Marioara, S.J. Andersen, W. Lefebvre, R. Holmestad, Philos. Mag. 94 (2013) 1-12.

[14] C. Ravi, Acta Mater. 52 (2004) 4213-4227.

[15] J. Svoboda, F.D. Fischer, P.H. Mayrhofer, Acta Mater. 56 (2008) 4896-4904.

[16] C. Laird, H.I. Aaronson, Acta Metall. 17 (1969) 505-519.

[17] K.T. Moore, J.M. Howe, Acta Mater. 48 (2000) 4083-4098.

[18] C.R. Hutchinson, X. Fan, S.J. Pennycook, G.J. Shiflet, Acta Mater. 49 (2001) 2827-2841.

[19] B.M. Gable, G.J. Shiflet, E.A. Starke, Metall. Mater. Trans. A 37A (2006) 1091-1105.

[20] Y. Weng, Z. Jia, L. Ding, K. Du, H. Duan, Q. Liu, X. Wu, Scripta Mater. 151 (2018) 33-37.

[21] S.J. Andersen, C.D. Marioara, R. Vissers, M. Torsæter, R. Bjørge, F.J.H. Ehlers, R. Holmestad, Mater. Sci. Forum 638-642 (2010) 390-395.

[22] J.M. Rosalie, H. Somekawa, A. Singh, T. Mukai, Philos. Mag. 90 (2010) 3355-3374.

Figure captions

Fig. 1. (a) TEM bright-field image of the Al-Mg-Si-Cu alloy aged at 170 °C for 1 month, (b) the HAADF-STEM image of cross-section of a β′ phase, (c) the corresponding FFT patterns of (b). The β′ unit cell and QP lattice are marked by red and green lines, respectively.

Fig. 2. (a, d, g, j) HAADF-STEM images of cross section of the rod-like β′ phases. (b, e, h, k) enlarged inverse FFT images of (a), (d), (g) and (j), respectively, (c, f, i, l) corresponding FFT patterns of (a), (d), (g) and (j), respectively. The β′ unit cells and QP lattice are marked by red and green lines, respectively.

Fig. 3. (a) HAADF-STEM image of cross-section of a rod-like β´ precipitate, (b-g) STEM-EDS maps of the precipitate in (a), (b) Al map, (c) Mg map, (d) Si map, (e) Cu map, (f) Fe map, (g) Mn map.

Fig. 4. (a, d) HAADF-STEM images of cross section of the lath-like β′ phases. (b, e) enlarged inverse FFT images of (a) and (d), respectively, and (c, f) corresponding FFT patterns of (a) and (d), respectively. The β′ unit cell is marked by red lines.

Fig. 5. (a) HAADF-STEM image of cross-section of a lath-like β´ precipitate, (b-g) STEM-EDS maps of the precipitate in (a), (b) Al map, (c) Mg map, (d) Si map, (e) Cu map, (f) Fe map, (g) Mn map.

Fig. 6. (a) and (d) HAADF-STEM images of cross section of the rod-like β′ phase and the lath-like β′ phase, respectively. (b) and (e) the close-up of the marked region in (a) and (d), respectively. (c) and (f) the corresponding illustration schematic of (b) and (e), respectively. The QP lattice is marked by green lines. The Cu atoms are marked by red circles.

Fig. 7. The β′-angle distribution of β′ phases in the over-aged Al-Mg-Si-Cu alloy.

Fig. 8. (a) Stereographic projection showing the location of the six ORs of β′ phases. (b) Statistics of the β′-angle of different β′ phases plotted as a function of the aspect ratio of cross-section of precipitates.

Fig.9. Schematic illustration of the interface between β´ phase and α-Al matrix.

Fig. 10. Schematic drawings of the relationship between the crystal structure of different phases and the QP lattice. The QP lattice is marked by blue dotted lines. The unit cell of various phases are marked by red and black lines.

Table captions

Table 1. Summary of the ORs of precipitates reported in Al-Mg-Si(-Cu) alloys.

Table 2. Lattice misfit between atomic rows and β′-angle.

Table 1. Summary of the ORs of precipitates reported in Al-Mg-Si(-Cu) alloys

Precipitate	Composition	Space group	Crystal parameters (nm)	Orientation relationship
β″	Mg_5Si_6	C2/m	a = 1.516, b = 0.405, c = 0.674, β = 105.3°	$(001)_{β''}$ // $(001)_{Al}$, $[100]_{β''}$ // $[310]_{Al}$ [4]
β′	Mg_9Si_5	$P6_3/m$	a = b = 0.715, c = 1.215, γ= 120°	$[001]_{β'}$ // $[001]_{Al}$, $[2\bar{1}\bar{1}0]_{β'}$ // $[\bar{3}10]_{Al}$ [5]
U1	$MgAl_4Si_5$	$P\bar{6}2m$	a = b = 0.405, c = 0.67	$(\bar{1}2\bar{1}0)_{U1}$// $(001)_{Al,}$ $[0001]_{U1}$^$[100]_{Al}$ = 20°[2]
	$MgAl_2Si_2$	$P\bar{3}m1$	a = b = 0.405, c = 0.674, γ = 120°	$[001]_{Al}$//$[100]_{U1}$, $[310]_{Al}$//$[001]_{U1}$, $[1\ 30]_{Al}$//$[120]_{U1}$ [6]
U2	$Mg_2Al_4Si_5$	Pnma	a = 0.675, b = 0.405, c = 0.794	$(001)_{U2}$// $(001)_{Al}$, $[010]_{U2}$^$[010]_{Al}$ = 20°[2]
	MgAlSi			$(001)_{Al}$// $(010)_{U2}$, $[\ 310]_{Al}$// $[100]_{U2}$, $[130]_{Al}$// $[001]_{U2}$ [3]
C	$Mg_4AlSi_{3.3}Cu_{0.7}$	$P2_1/m$	a = 1.032, b = 0.81, c = 0.405, γ = 101°	$(001)_C$ // $(001)_{Al}$, $[100]_C$ // $[100]_{Al}$ [9]
Q′	$Al_4CuMg_6Si_6$	$P\bar{6}$	a = b = 1.04, c = 0.405	$[0001]_{Q'}$ // $[001]_{Al}$, $[1\bar{2}10]_{Q'}$ // $[130]_{Al}$ [9] Multiple orientation relationships [11]
Q	$Al_4Cu_2Mg_8Si_7$	$P\bar{6}$	a = b = 1.039, c = 0.402	$[0001]_Q$ // $[001]_{Al}$, $[\bar{1}\bar{1}20]_Q$ // $[510]_{Al}$ [9]
	$Al_5Cu_2Mg_8Si_6$	Hexagonal	a = b = 1.03, c = 0.4505	Six different orientation relationships [10]

Table 2. Lattice misfit between atomic rows and β′-angle.

OR	Parallel directions	β´-angle	Distance between two atomic rows (nm)		Misfit	Anisotropic misfit values
0	$<2\bar{1}\bar{1}0>_{β'}$//$<1\bar{3}0>_α$	~11.6°	$D_{<2\text{-}1\text{-}10>β'}$=0.619	$D_{<1\text{-}30>α}$=0.640	3.28%	5.31%
	$<10\bar{1}0>_{β'}$//$<310>_α$		$5D_{<10\text{-}10>β'}$=1.170	$2D_{<310>α}$=1.280	8.59%	
	$[0001]_{β'}$//$[001]_α$					
1	$<2\bar{1}\bar{1}0>_{β'}$//$<4\bar{9}0>_α$	~6.1°	$3D_{<2\text{-}1\text{-}10>β'}$=1.857	$D_{<4\text{-}90>α}$=1.994	6.87%	0.75%
	$<10\bar{1}0>_{β'}$//$<940>_α$		$8D_{<10\text{-}10>β'}$=1.872	$D_{<940>α}$=1.994	6.12%	
	$[0001]_{β'}$//$[001]_α$					
2	$<2\bar{1}\bar{1}0>_{β'}$//$<3\bar{8}0>_α$	~9.4°	$3D_{<2\text{-}1\text{-}10>β'}$=1.857	$D_{<3\text{-}80>α}$=1.730	6.84%	1.52%
	$<10\bar{1}0>_{β'}$//$<830>_α$		$7D_{<10\text{-}10>β'}$=1.638	$D_{<830>α}$=1.730	5.32%	
	$[0001]_{β'}$//$[001]_α$					
3	$<11\bar{2}0>_{β'}$//$<9\bar{2}0>_α$	~12.5°	$3D_{<11\text{-}20>β'}$=1.857	$D_{<9\text{-}20>α}$=1.867	0.54%	5.62%
	$<1\bar{1}00>_{β'}$//$<290>_α$		$4D_{<1\text{-}100>β'}$=1.752	$D_{<290>α}$=1.867	6.16%	
	$[0001]_{β'}$//$[001]_α$					
4	$<11\bar{2}0>_{β'}$//$<4\bar{1}0>_α$	~14.1°	$4D_{<11\text{-}20>β'}$=2.476	$3D_{<4\text{-}10>α}$=2.505	1.16%	3.52%
	$<1\bar{1}00>_{β'}$//$<140>_α$		$2D_{<1\text{-}100>β'}$=0.876	$D_{<140>α}$=0.835	4.68%	
	$[0001]_{β'}$//$[001]_α$					
5	$<2\bar{1}\bar{1}0>_{β'}$//$<100>_α$	~0°	$2D_{<11\text{-}20>β'}$=1.238	$3D_{<100>α}$=1.215	1.86%	11.47%
	$<10\bar{1}0>_{β'}$//$<010>_α$		$3D_{<10\text{-}10>β'}$=0.702	$2D_{<010>α}$=0.810	13.33%	
	$[0001]_{β'}$//$[001]_α$					

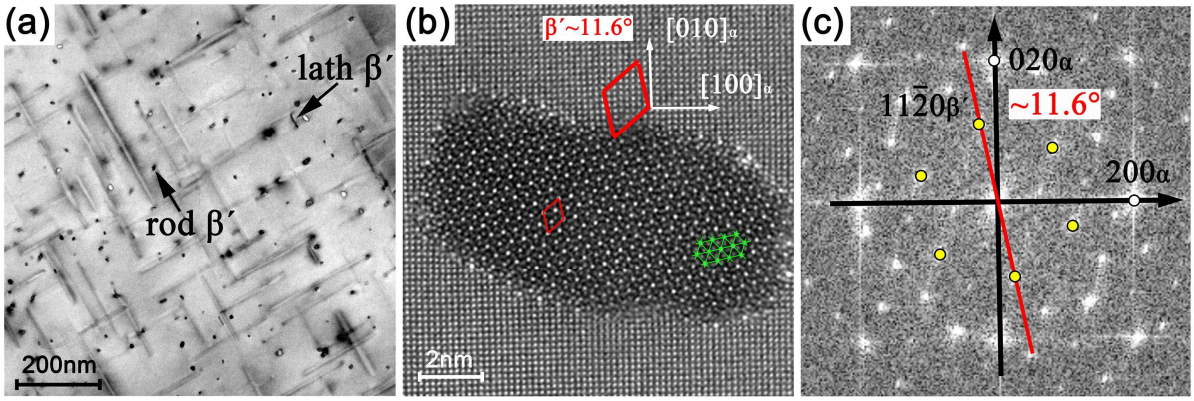

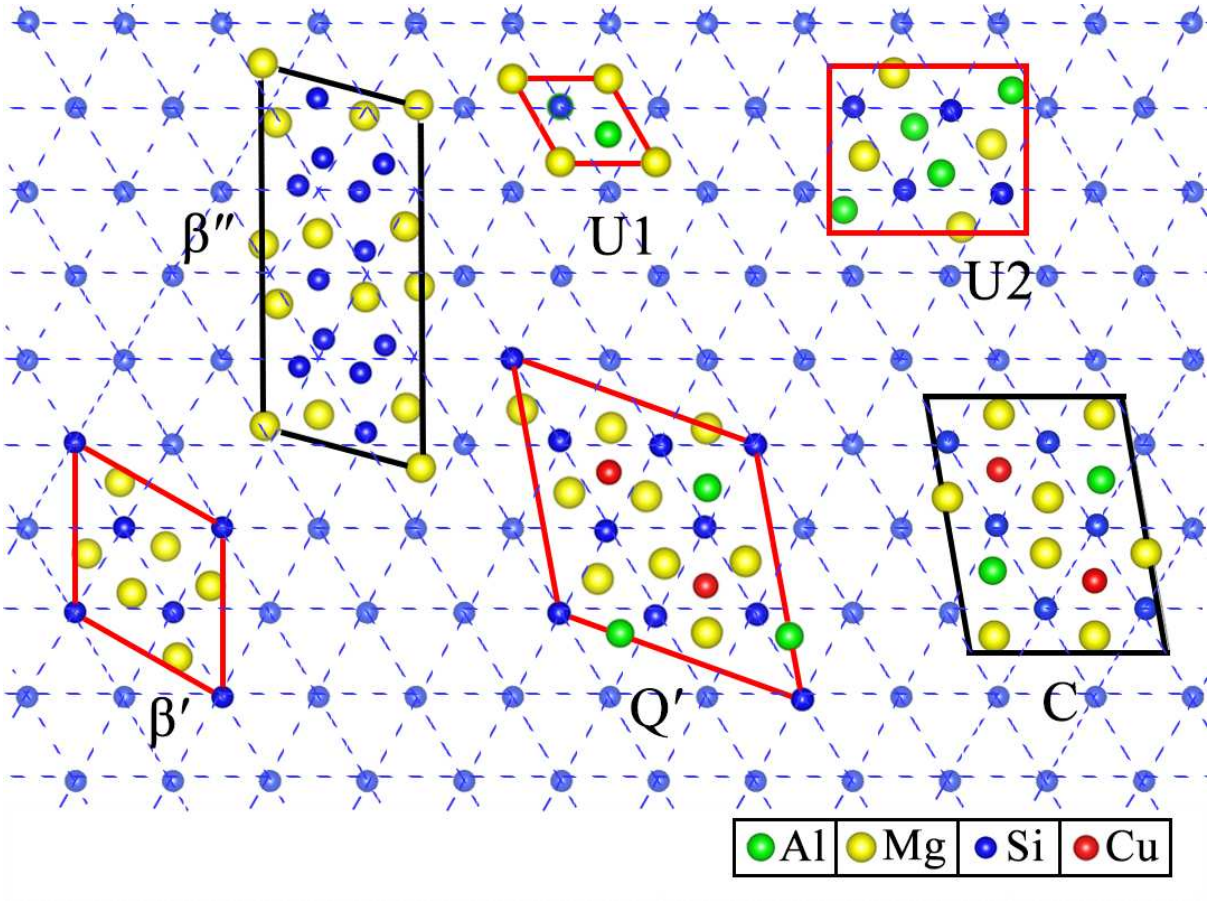

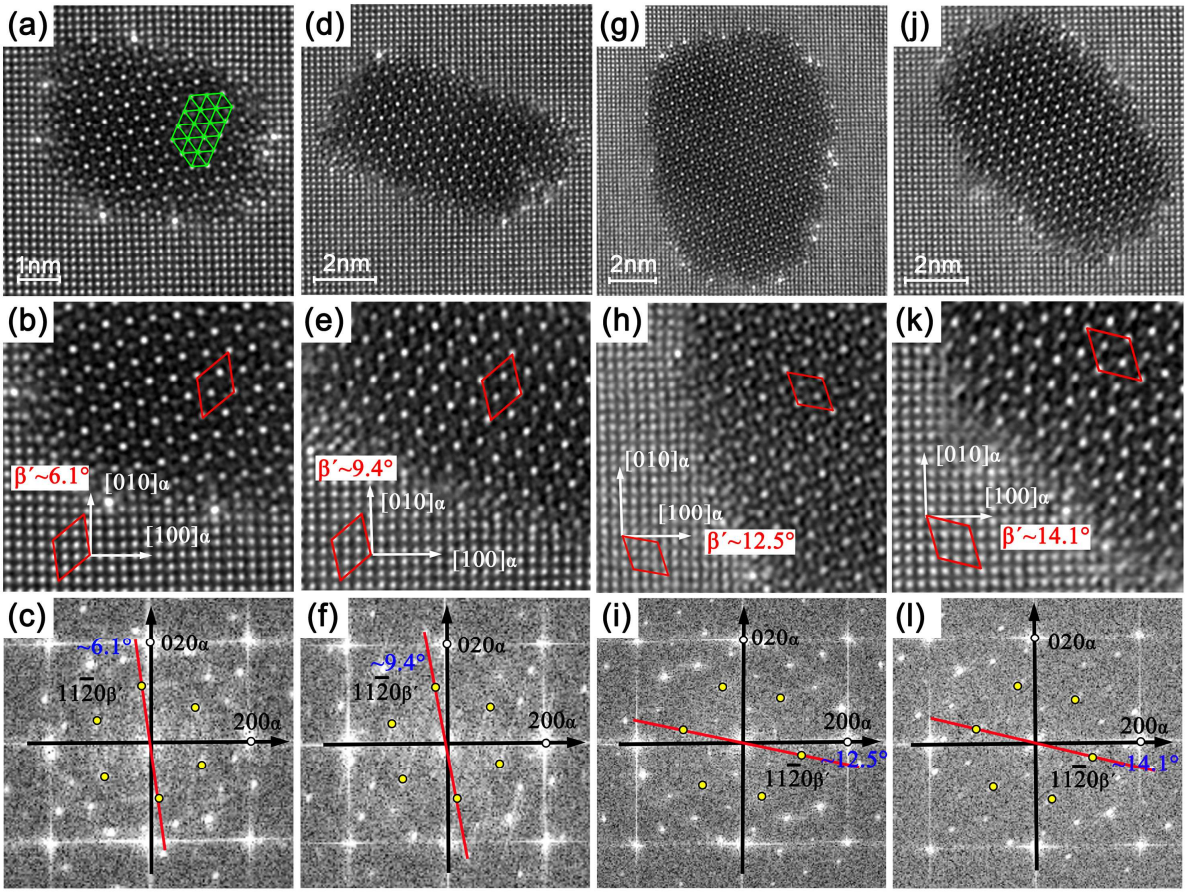

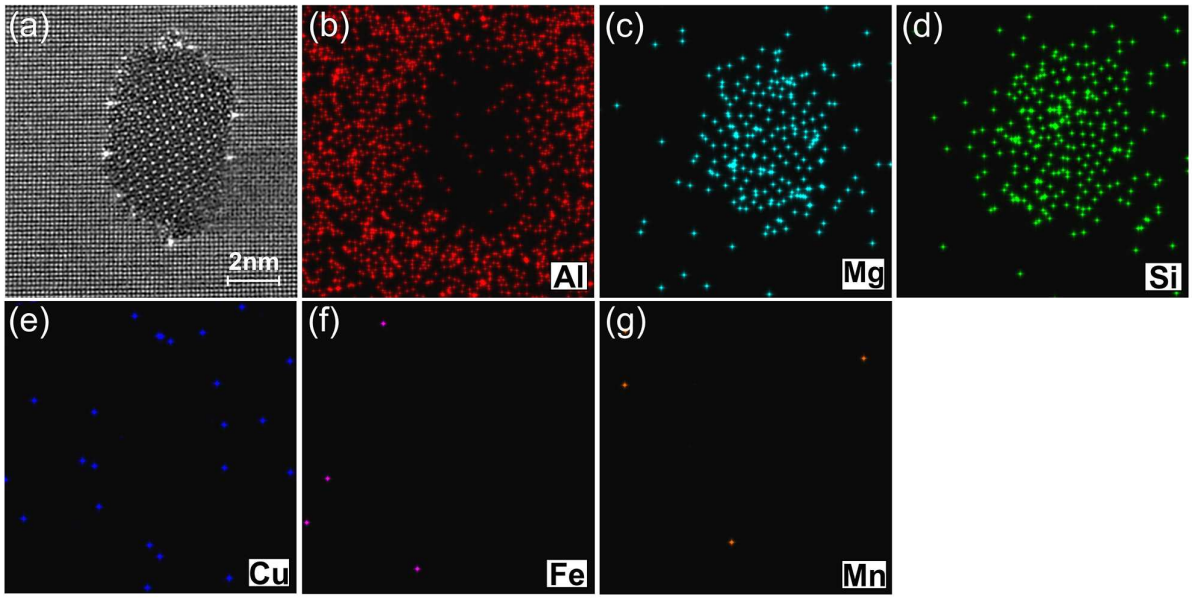

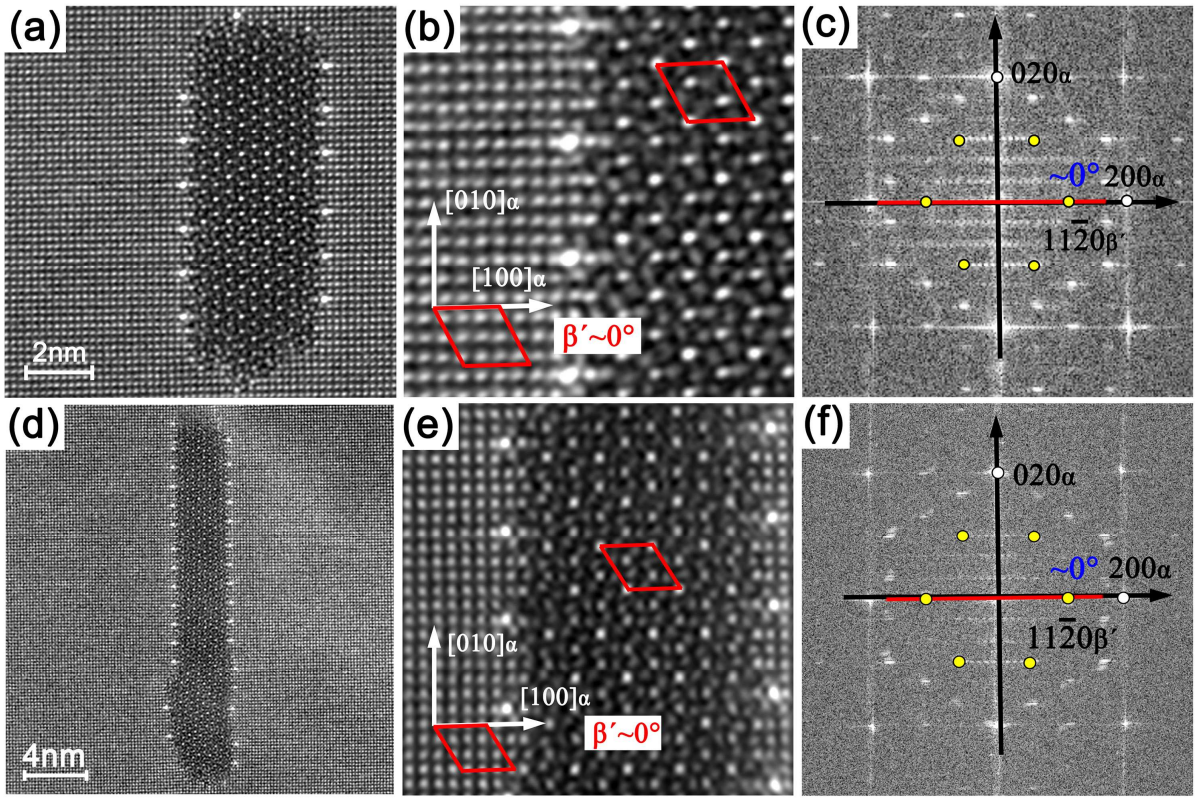

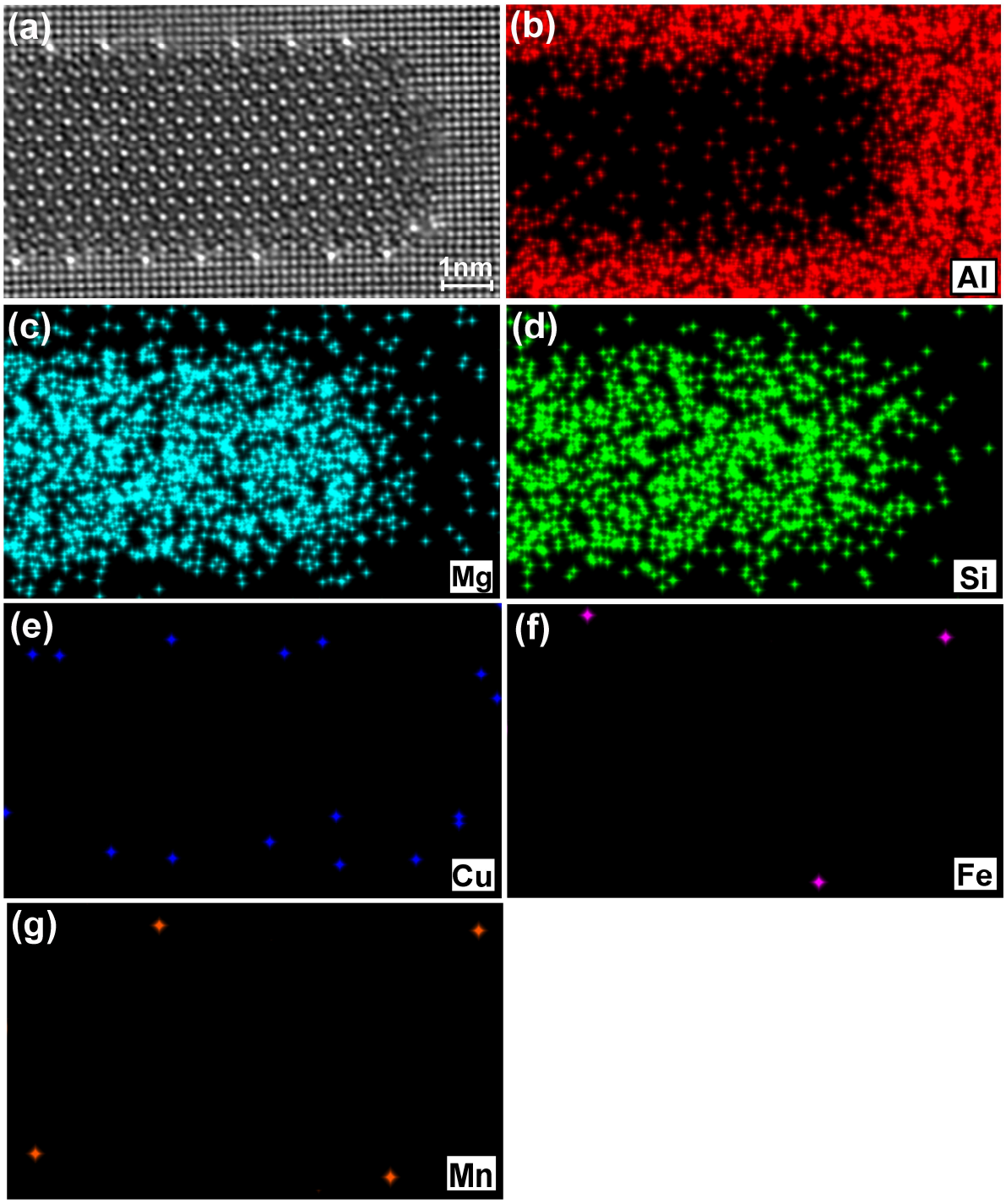
(a)
1nm
(b)
Al
(c)
Mg
(d)
Si
(e)
Cu
(f)
Fe
(g)
Mn

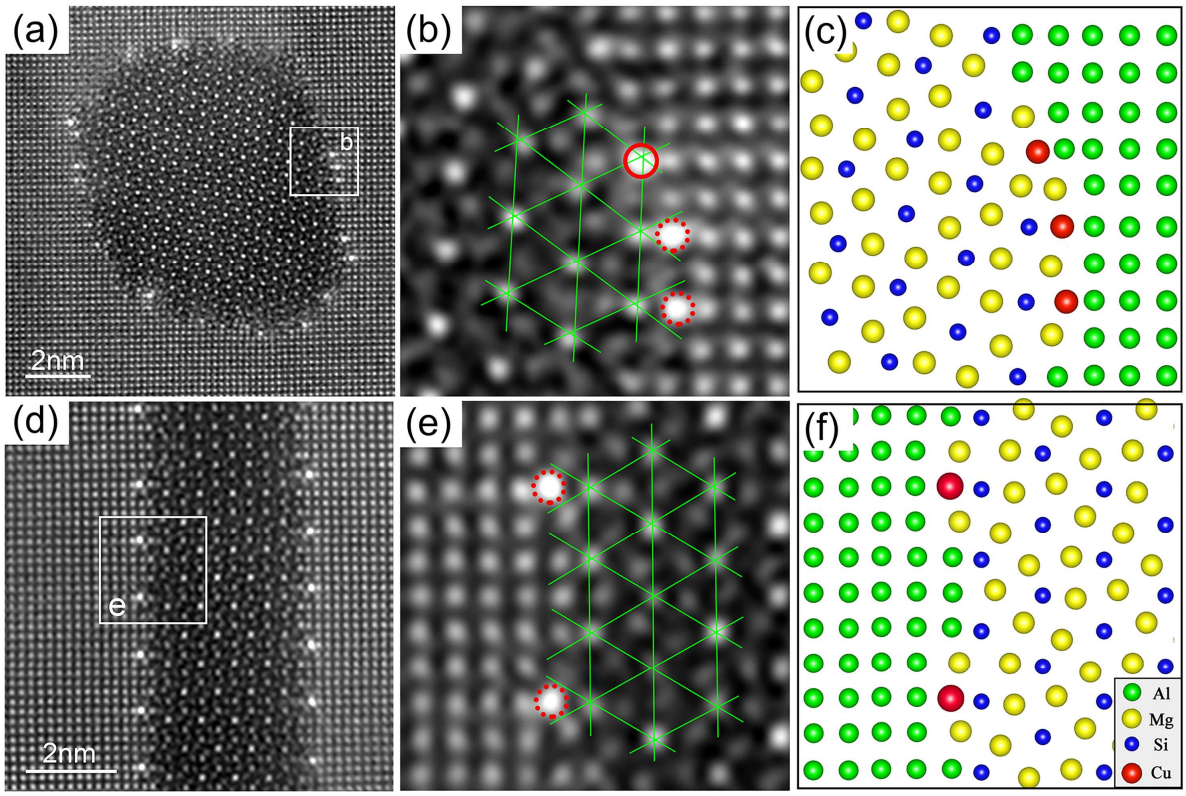

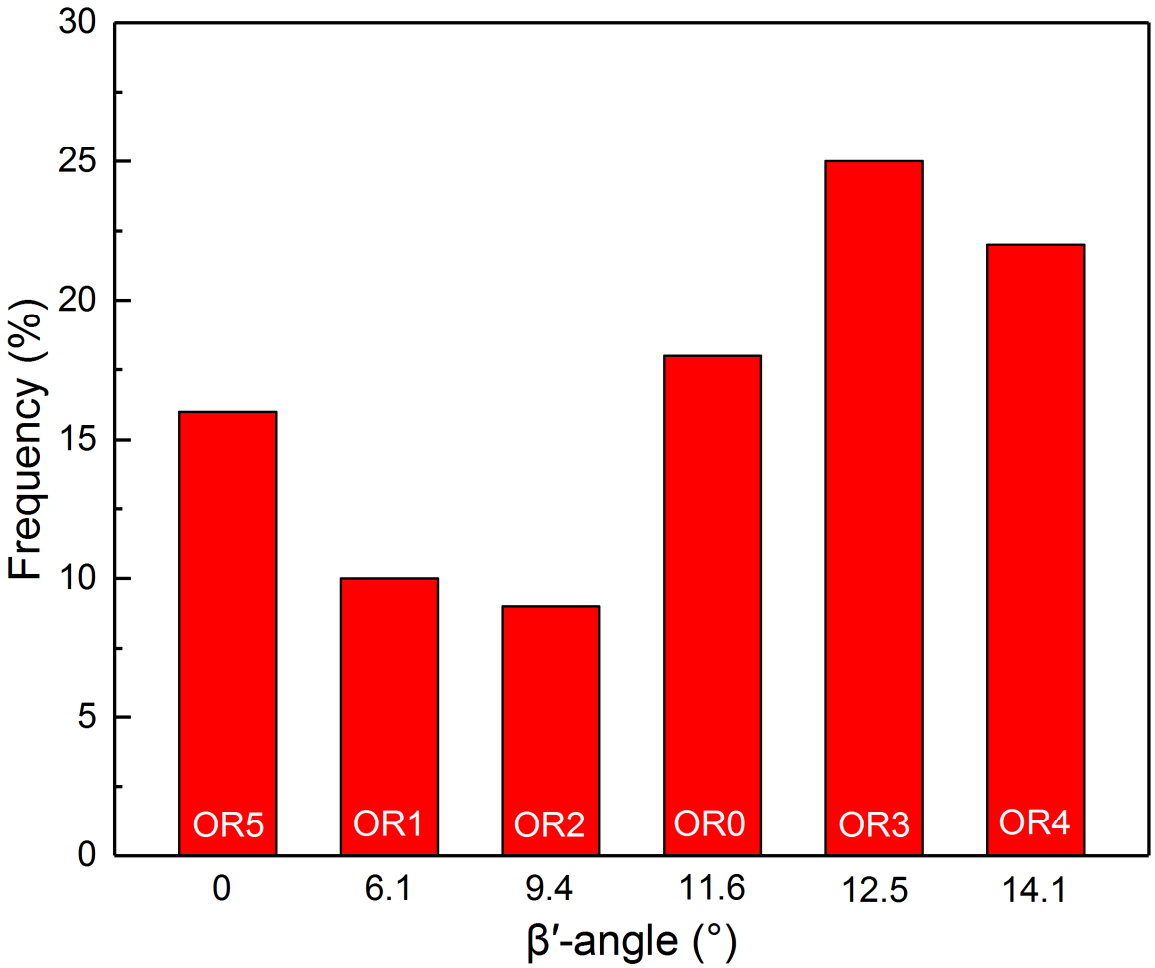
30
25
20
15
10
5
0
Frequency (%)
OR5
OR1
OR2
OR0
OR3
OR4
0
6.1
9.4
11.6
12.5
14.1
β′-angle (°)

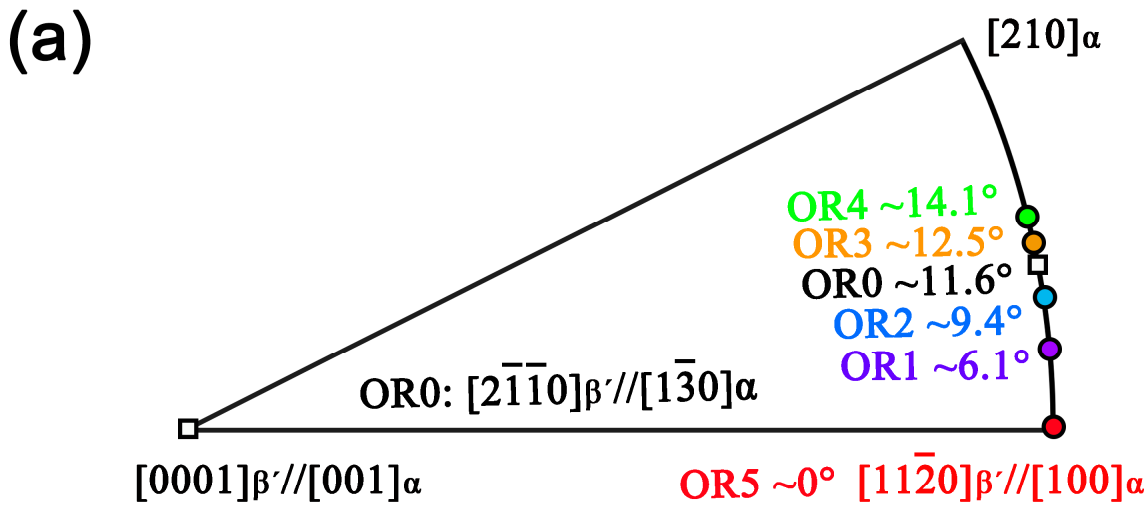
(a)
[210]α
OR4 ~14.1°
OR3 ~12.5°
OR0 ~11.6°
OR2 ~9.4°
OR1 ~6.1°
OR0: [2$\bar{1}\bar{1}$0]β′//[1$\bar{3}$0]α
[0001]β′//[001]α
OR5 ~0° [11$\bar{2}$0]β′//[100]α

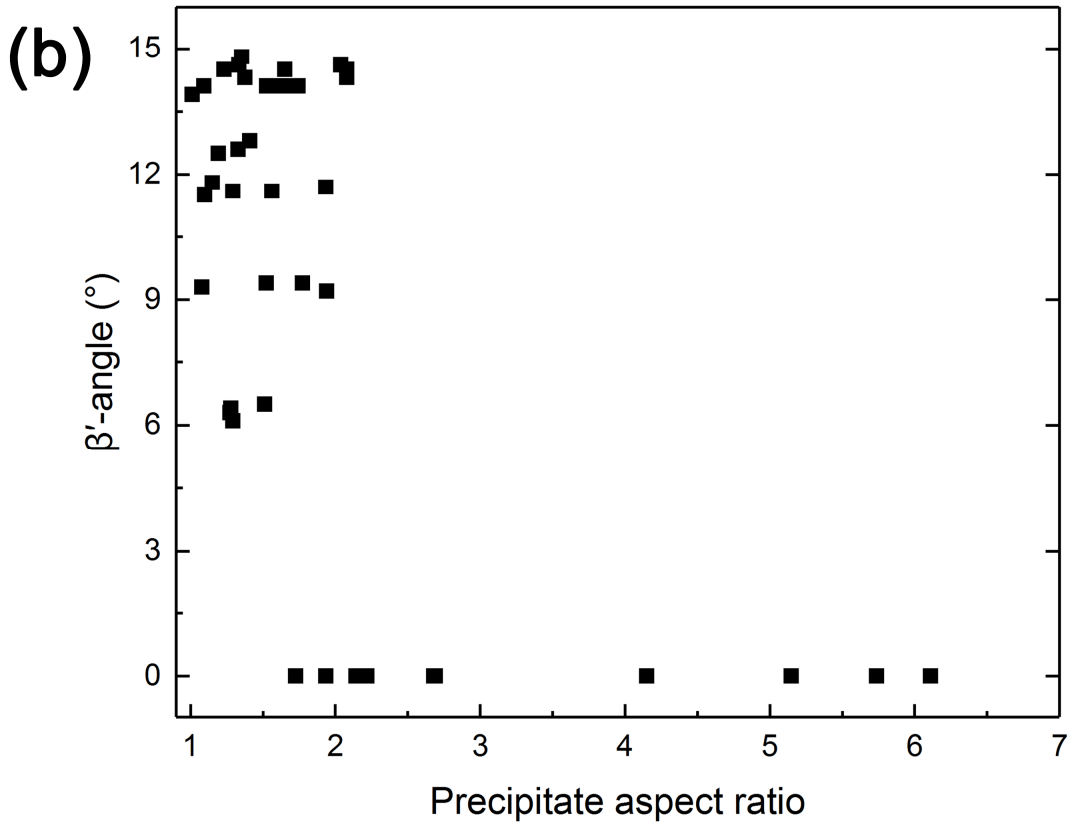
(b)
β′-angle (°)
0
3
6
9
12
15
1
2
3
4
5
6
7
Precipitate aspect ratio

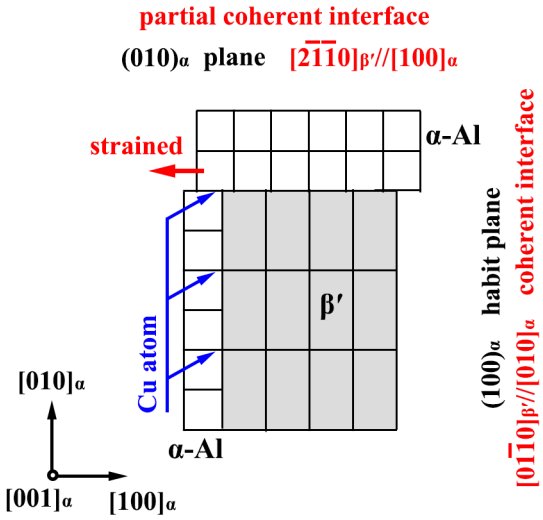

Highlights

- Six different ORs and two morphologies are revealed for β′ precipitates.
- The multiple ORs of β′ are attributable to the rotation of QP lattice.
- Cu segregation is observed at the β′/α-Al interfaces.